Influence of gold particle size in Au/C catalysts for base-free oxidation of glucose

C. Megías-Sayago[1 *], J. L. Santos[1], F. Ammari[2], M. Chenouf [1,2], S. Ivanova[1], M. A. Centeno[1], J. A. Odriozola[1]

[1] Instituto de Ciencia de Materiales de Sevilla, Departamento de Química Inorgánica, Universidad de Sevilla-CSIC, Américo Vespucio 49, 41092, Sevilla, Spain

[2] LGPC, Department of Chemical Process Engineering, Farhat-Abbas Sétif-1 University, Setif, Algeria

* Corresponding author: cristina.megias@icmse.csic.es

Abstract

A series of gold colloids were prepared and immobilized on commercial activated carbon. The influence of the colloid preparation and stability were studied and related to the gold particle size in the final catalyst. The catalysts show an important activity in the glucose to gluconic acid oxidation reaction, leading to gluconic acid yield close to 90% in base free mild conditions (0.1 MPa O_2 and 40ºC). The size-activity correlation and probable mechanism were also discussed. Finally, the viability of the catalyst was tested by recycling it up to four times.

Keywords: gold catalysts, carbon-supported catalysts, glucose oxidation, liquid-phase oxidation, biomass conversion

1. Introduction

Biorefinery, defined as the efficient transformation of renewable materials to fuels and intermediate chemicals, and associated to environmental and economic benefits, has driven the research in this area to notable increase in the last decades [1–4]. Within the renewable materials the vegetal biomass, mostly constituted by carbohydrates, represents around 75% of the total renewable biomass [5]. Among the carbohydrates represented in this biomass the cellulose remains the most attractive fuel precursor, mainly due to its low price, chemical purity and because it is formed only by one monomer – glucose [6]. After cellulose depolimerazion the subsequent transformation of glucose to valuable compounds involves a variety of processes such as hydrogenation [7], isomerization [8], dehydration [9] and oxidation [10]. Every single mentioned process or a combination of them lead to the formation of different 'platform chemicals'. As an example, the D-Gluconic acid, derived from the oxidation of glucose at anomeric position, results to be an useful food additive and raw material for drugs and biodegradable polymers manufacturing [11,12]. Industrially D-Gluconic acid is produced by enzymatic fermentation process [13,14] for which the principal inconvenient for sustainable large-scale production is the necessity of a neutralization step in order to avoid enzymes deactivation by the produced acid [15]. This problem could be solved either by using a base or by the substitution of the enzymes with a heterogeneous catalyst able to oxidize glucose under mild base-free conditions by using either O_2 or H_2O_2 as oxidants [16–19].

Although the use of base (NaOH and a relatively high pH of around 9-9.5) results in increase of heterogeneous catalyst's activity due to particle size stabilization and metal leaching suppression [20–22], a decrease in the selectivity to gluconic acid is often observed caused by the glucose to fructose isomerization process [23]. In addition, the formation of gluconate salt instead of pure gluconic acid occurs and entails the need of

cost effective post-reaction treatment to obtain the target acid. Therefore, a simple base-free heterogeneously catalyzed process able to produce selectively gluconic acid and avoiding the problems of particle size sintering and metal leaching is highly desirable.

Within the catalyst's candidates for such a process, the most promising alternative is nanometric gold. Glucose oxidation has been carried out over both unsupported [24,25] and supported [20,26] gold catalysts with good results in activity and selectivity; however, some issues must be addressed in order to improve the catalytic system. Various studies reported the base-free aerobic oxidation of glucose over gold supported catalysts with good results in activity and selectivity [22,27–29]. Most authors found a clear dependence of glucose oxidation activity on average gold particle size, suggesting that the oxidation proceeds directly on gold metal surface rather than on the contact perimeter between gold and support [26,28,30]. On the other side, it is still under debate the optimal gold particle size and if the nanoparticle shape plays any significant role in oxidation process. A serious inconvenient for the use of supported nanogold catalysts in the base-free glucose oxidation is related to the possible metal leaching and/or the gold sintering during the reuse cycles, driving to loss of activity [29]. The latter suggests the importance of adequate choice of support, able to stabilize the gold particles thus avoiding the leaching/sintering phenomena.

Most of the studied supports are simple or mixed metal oxides such as TiO_2 [27], MgO [31] Al_2O_3, CeO_2, CeO_2(25wt%)/ZrO_2, CeO_2(50wt%)/ZrO_2 and CeO_2(20wt%)/Al_2O_3 [29]. The use of carbon supports has been also widely reported [32–36]. No matter the type of carbon supports i.e., activated carbon, carbon nanotubes or carbon nanofibers, Au/C systems showed high activity and selectivity in the oxidation of glucose [22,37,38].

In general, the substantial importance of active carbon as metal support in industrial catalysis is well recognized. Its stability in both acidic and basic media, its tunable pore structure and stability at high temperatures, the easiness of metal phase recovery by carbon burn away and its lower costs in comparison with conventional supports such as alumina and silica [39,40] convert it in a versatile material for heterogeneous catalysis. The real relevance of carbon in aqueous-phase oxidation reactions derived from its hydrophobicity, which usually difficults active metal phase leaching, thus improving catalyst's inherent activity. In fact, higher activity of hydrophobic catalysts in glucose oxidation compared to hydrophilic catalysts application has been reported [41,42]. This difference in activity was assigned to stronger adhesion between hydrophobic catalyst grains and oxygen bubbles leading to an increase of the catalyst grains number at the gas-liquid interface and, therefore, to an increase in the rate of the gas transfer towards the catalysts [38]. The only disadvantage of using hydrophobic support is that the conventional methods for gold nanoparticles preparation, such as deposition-precipitation or direct anionic exchange are less useful resulting in important gold loss and low reproducibility. Within the existing gold nanoparticles preparation methods, the gold colloidal route seems the most appropriated to obtain a homogeneous and reproducible gold nanoparticles size distribution which allows a more direct gold size/activity correlation. Nevertheless, the use of the colloidal route for preparing Au/C samples includes the utilization of particles stabilizing agents as citrates, polyvinyl alcohol (PVA) etc. which if not removed from the gold surface could influence the measured activity due to some shielding effects [30]. It is important therefore to remove any rests of stabilizing agents in order to observe the "real" size/activity effect on the reaction of glucose oxidation.

From all above, the aim of this work is to gain insights into the role of gold particle size and shape in the base free oxidation of glucose to gluconic acid. For that, a series of Au/C catalysts with different gold particle size were prepared and their catalytic performances evaluated in the oxidation reaction. The catalysts resulted from immobilization of gold colloids with different gold sizes on a commercial activated carbon, and were subjected to a calcination treatment at 300 ºC in order to remove any precursor leftovers and to stabilize the gold nanoparticles onto the carbon surface in order to assure as much as possible the permanence of the gold size during the reaction course. The evaluation of the catalyst's reusability was also undertaken.

2. Experimental

2.1. Synthesis

Activated charcoal powder DARCO® (Sigma Aldrich, 100 mesh particle size) and $HAuCl_4$ (Johnson Matthey) gold precursor were used as received.

The deposition of gold (2 wt.% nominal value) on the carbon support was carried out according to the colloidal method assisted by polyvinyl alcohol (PVA) where $NaBH_4$ (Sigma Aldrich) was used as reducing agent [43]. The necessary amount of gold precursor was dissolved in water to a final concentration of 5.10^{-4} M and the corresponding quantity of PVA (1% wt. aqueous solution) was added and stirred during 20 min. After that, the appropriate amount of 0.1M freshly prepared $NaBH_4$ solution was quickly added to reduce the gold precursor. After 20 min stirring, sample of 5 mL was taken to characterize the colloid and the rest of solution was put in contact to the adequate amount of the commercial activated carbon in order to have a theoretical gold loading of 2%wt. 45 min later, the final mixture was centrifuged at 15000 rpm for 20 minutes in order to ensure the anchorage of the totality of gold nanoparticles on carbon. The resulted samples were

filtered and dried at 100 ºC for 2 hours and finally calcined at 300 ºC for 2 hours. Following this procedure, 11 samples, were prepared as a function of PVA:Au weight ratio (Series 1) and $NaBH_4$:Au molar ratio (Series 2). The Table 1 summarizes the synthesis parameters of both series of gold samples. Gold colloids and their corresponding catalysts were named as 'Col X' and 'AuC X' respectively, being X a distinctively roman number of order.

Table 1. Code and Au/PVA/$NaBH_4$ ratios of the prepared gold samples

	Sample	PVA:Au ratio[a]	$NaBH_4$:Au ratio[b]
Series 1	Col I / AuC I	0	5
	Col II / AuC II	0.5	5
	Col III / AuC III	**0.85**	**5**
	Col IV / AuC IV	3	5
	Col V / AuC V	5	5
	Col VI / AuC VI	10	5
Series 2	Col VII / AuC VII	0.85	0.5
	Col VIII / AuC VIII	0.85	1
	Col IX / AuC IX	0.85	2
	Col X / AuC X	0.85	3
	Col III / AuC III	**0.85**	**5**
	Col XII / AuC XII	0.85	10

[a] Weight ratio, [b] molar ratio

2.2 Characterization Techniques

UV-Vis measurements were carried out on UV-Vis Avantes AvaLight-DH-S-BAL spectrometer equipped with optic fiber liquid sensor for wavelengths ranged from 100 to 1000 nm.

XRD measurements were performed at room temperature on Panalitycal X'Pert Pro diffractometer, equipped with Cu anode with 0.05° step size and acquisition time of 300 s

in 10-90° 2θ range. The average gold crystallite size of the Au/C catalysts was calculated from the broadening of the (111) Au plane at 38.28º 2θ applying Scherrer's equation.

Transmission electron microscopy (TEM) micrographs were acquired on PHILIPS CM-200. The mean gold particle diameter was considered on the basis of its homogeneity, degree of dispersion and number of particles. The average gold particle size was estimated considering the surface distribution calculation, expressed in equation 2.

$$D\,[3,2]=\frac{\sum_1^n D_i^3 v_i}{\sum_1^n D_i^2 v_i} \qquad (2)$$

where D_i is the geometric diameter of the i^{th} particle, and v_i the number of particles with this diameter. For every distribution the total number of measured particles overcomes 200 particles per sample (colloid or catalyst).

The gold loadings were estimated through ICP analysis by using Horiba Jobin Yvon spectrometer after fluorhydric acid digestion of the samples.

2.3 Catalytic tests

Aerobic oxidation of glucose (D-(+)-Glucose anhydrous, 99%, from Alfa Aesar) was carried out in a glass batch reactor (50 mL) equipped with Young valve, magnetic stirrer and saturated with oxygen at atmospheric pressure (P_{O2} approximately 0.1 MPa). In a typical experiment, the reactor was charged with a 0.2M glucose solution, catalyst in Glucose/Au molar ratio of 100 and oxygen, in the aforementioned order. The oxygen diffusion through solution was assured by 20 mL/min pure oxygen flux bubbling for few minutes. Afterwards, the reactor was closed and the mixture stirred at 600 rpm, at 40ºC during 18 hours in base-free conditions. Once the reaction finished, 500 µL of sample

taken from the final reaction mixture and diluted in 500 µL of ultra-pure water was immediately analyzed by HPLC. The products of glucose oxidation were identified and quantified by using a Hi-Plex H column (300 × 7,7 mm), a refractive index detector (Varian 360-LC) and MilliQ water as mobile phase. Glucose conversion was calculated as described by equation (1).

$$Conversion\ (\%) = \frac{[Glucose]_i - [Glucose]_f}{[Glucose]_i} \qquad (1)$$

3 Results and discussion

3.1. Colloids characterization

The influence of PVA:Au and $NaBH_4$:Au ratios on gold particle size and morphology was studied by both UV-Vis spectroscopy and TEM microscopy. Figure 1 presents the UV-Vis absorption spectra of all synthesized colloids. All samples present an intense absorption with maxima in the 502-530 nm region. This absorption is characteristic of the surface plasmon resonance of Au metal fine particles and its position, intensity and width is strongly dependent on the size and shape of the Au particles, as well as of the dielectric properties of the surrounding environment [44].

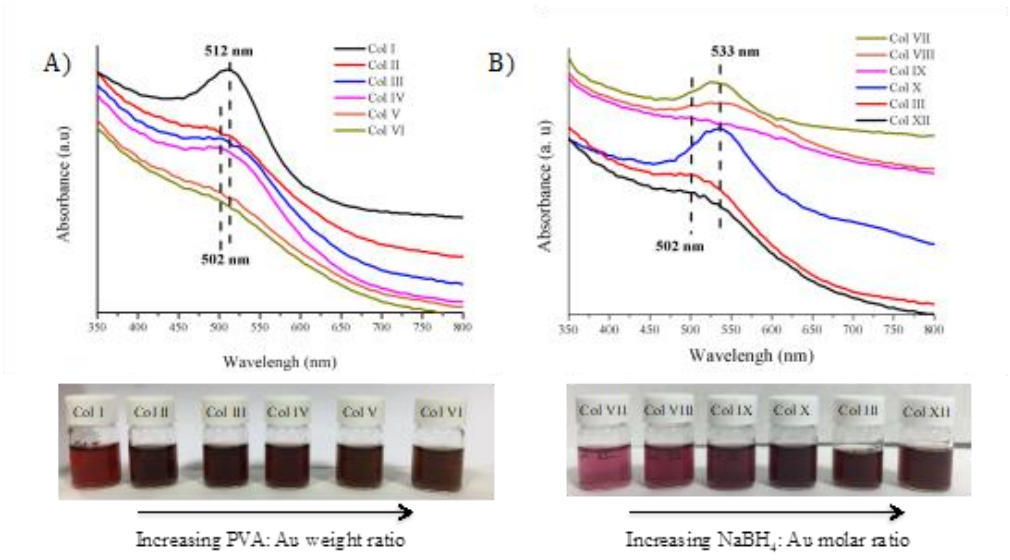

Figure 1. UV-Vis spectra of gold colloids. A) Series 1, B) Series 2

For both colloidal series, a modification in the position, shape and width of the gold plasmon band is observed from one colloid to another, indicating differences in the average gold particle size and/or morphology. In good agreement, changes in the color of the colloidal solutions are also observed (see figure 1), all of them in the reddish mauve spectra. The color of gold colloids is also indicative for the resulted gold particles size and depends on support (if used), on gold concentration, morphology and size distribution [45]. In particular, colloidal gold is red when the corresponding particles are smaller than 20 nm. So far from the color we can deduce that our gold particles independently on the synthetic parameters present sizes always below/around 20 nm.

From figure 1A is obvious that increment in PVA:Au ratio during the preparation leads to blue shift of around 10 nm in the position of the gold plasmon which can be related with the formation of smaller nanoparticles. This size variation was also confirmed by TEM (Figure 2) and the calculated average gold particle size decreases constantly from 3.6 nm (Col I) to 1.8 nm (Col VI) with the increase of the PVA concentration for series 1 (Table 2). In all cases, the obtained particle shape is similar, as deduced from the particle size distributions and TEM micrographs.

It is well known, that the final particles size is based on a fine balance between the velocity of nucleation and particle growth, which by themselves could be controlled by changing the nanoparticles' synthesis parameters. There exist many theories explaining the mechanisms of nucleation and growth of the metal nanoparticles. The velocity of gold nanoparticles nucleation and growth generally depends on the pH of the solution, on the reducing agent nature and concentration and on the presence of surfactants [46]. Ji et al. [47] reported that the pH dependence could be ascribed to the existence of differently hydrolyzed gold complexes and their reactivity towards reducing agent. When a very diluted gold precursor solutions (as in our case) are employed, the pH of the solution

neighbors that of distilled water (6-6,5). At this pH, Ivanova et al. [48] reported that the 70 % of Au could be found as $[Au(OH)_2Cl_2]^-$ and $[Au(OH)_3Cl]^-$ complexes. These complexes get reduced with slower nucleation time (60 s) than the less hydrolyzed ones and show lower growth velocity. The nature of the reducing agent is also very important, stronger the reductive potential of the agent lower the time of nucleation. The use of $NaBH_4$ indicates quasi-instantaneous nucleation within a few seconds to an average radius of 2 nm which then undergo coalescence up to 4 nm [49] in the first 20 min, the case of Col I when no stabilizing agent is used. The fast nucleation of gold could be then considered as separate processes from the particle size growth which will depends primarily on colloidal stability, i.e. on the increase of the aggregation barrier [46]. The later could be achieved by the use of stabilizing agent (PVA in our case). Indeed the stability of the colloidal solution as a function of time showed interesting differences between the samples. Whereas Col I and II samples agglomerate and precipitate after two days, the Col III to VI remain stable. The correlation between colloid stability and gold particle size suggests that stable gold colloids could be obtained at PVA/Au ratios superior to 0.85 with resulting particle size of 2.3±0.5 nm. Because of this observation, the series 2 (Col VII to Col XII colloids) was prepared at a fixed PVA:Au ratio of 0.85 and varying the $NaBH_4$:Au proportion.

For this series, the increment of the $NaBH_4$:Au ratio also leads to a blue shift of the gold plasmon (see Fig. 1B), pointing out the formation of smaller nanoparticles at high concentration of the reductant agent (Table 2). However, the TEM analysis (figure 2) put in evidence that the variation $NaBH_4$:Au ratio affects also the shape and size heterogeneity of the produced gold nanoparticles. Thus, at low ratios (low concentration of reductant agent) a wide particle size distribution is obtained, generating gold particles from 7 to 25 nm and resulting in higher average particle size. Besides this, a change of

particles morphology from spherical to triangular and/or irregular shapes is evidenced. Narrower particles size distribution and lower mean particle size were observed with the increase of the $NaBH_4$ /Au ratio. For Col IX an important contribution of particles in the 1 - 5 nm range is observed, with very few agglomerates. $NaBH_4$ /Au ratio of 3 seems to be the limiting value above which stable colloids of gold particles of 2.3 nm are obtained.

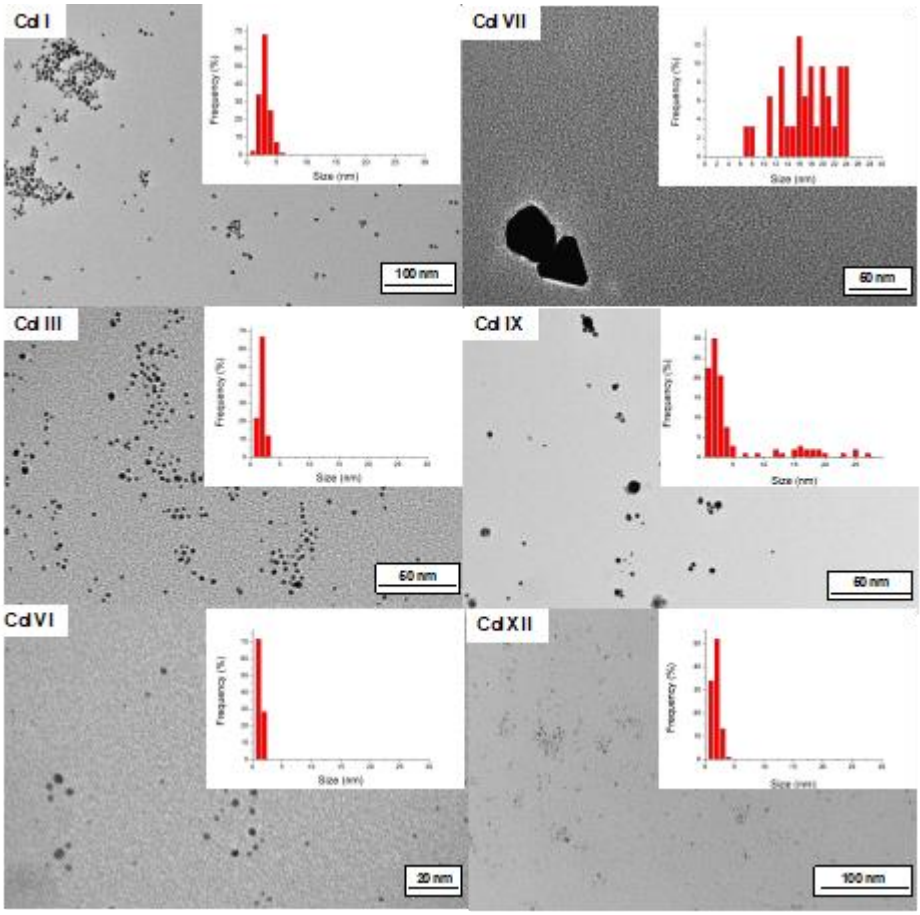

Figure 2. Representative TEM micrographs and gold size distribution for selected prepared gold colloids

Table 2. Average gold particle size of the prepared colloids

	Sample	Average particle size (from TEM), nm
Series 1	Col I	3.6
	Col II	3.3
	Col III	**2.3**
	Col IV	2.8
	Col V	2.3
	Col VI	1.8
Series 2	Col VII	18.9
	Col VIII	3.7
	Col IX	7.6
	Col X	4.9
	Col III	**2.3**
	Col XII	2.2

3.2 Au/C Catalysts

The pre-formed colloids were immobilized on activated carbon targeting Au loading of 2 wt.%. After the calcination treatment (300ºC, 2h), no significant modification of the textural properties of the parent carbon support was observed. Diffuse Infrared Fourier Transform Spectroscopy (DRIFTS) study evidenced total removal of the PVA protective layer on the surface of the gold nanoparticles (figure not shown). The real gold loadings measured by ICP are summarized in Table 3.

The deposited amount of gold is slightly over 2wt.% in majority of the samples indicating the successful immobilization of the colloid on carbon surface. However, for the samples prepared with the highest PVA/Au ratios (Au/C V and Au/C VI), a lower gold uptake is produced, in such a way that higher the PVA/Au ratio used for the colloid formation, lower the immobilized gold loading. Considering that, the stability of the colloids is proportional to the PVA concentration the anchoring of gold could become more difficult and responsible for the lower gold uptake. From here, and despite the low average gold particle size obtained for these colloids, PVA/Au ratios higher than 3 must be avoided in order to assure total immobilization of the gold nanoparticles.

Table 3. Experimental gold loadings, mean Au particle size, dispersion and TOF of the supported gold catalysts.

	Sample	% Au [ICP]	Average particle size (from TEM), nm	Average particle size (from XRD), nm	Dispersion (%)	TOF, $s^{-1}*10^3$
Series 1	AuC I	2.0	15.4	14.9	10	11.24
	AuC II	2.3	9.3	9.3	15	7.08
	AuC III	2.4	8.7	10.4	16	6.19
	AuC IV	2.3	10.1	11.1	14	5.60
	AuC V	1.1	6.8	6.6	20	7.58
	AuC VI	0.5	4.1	4.4	32	8.59
Series 2	AuC VII	2.1	22.8	28	7	9.40
	AuC VIII	2.3	20.1	25.4	7.5	12.04
	AuC IX	2.3	22.2	22.5	7	14.5
	AuC X	2.2	20.4	16.1	7.4	14.7
	AuC III	2.4	8.7	10.4	16	6.19
	AuC XII	2.3	4.8	5.2	27	3.77

The average gold particle sizes of the supported gold samples were calculated from both TEM and XRD measurements (Table 3) and present similar trends to those of the parent colloids. Figure 3 shows representative TEM micrographs and gold particle size distribution for the Au/C samples.

For all samples, an 3 to 4 fold increase of the gold particles size was observed, which can be assigned to particles agglomeration occurred after the thermal treatment carried out in the supported catalysts (calcination at 300 ºC for 2 hours). An almost linear correlation was found between the metal particle size in the colloids and in the corresponding supported solid (Figure 4), being only the sample corresponding to the Col VII pulled apart of the tendency due to the already aggregated state obtained in the initial colloid.

On the other hand, a good linear relationship was also achieved between the average gold particle size determined by TEM and XRD (Figure 5).

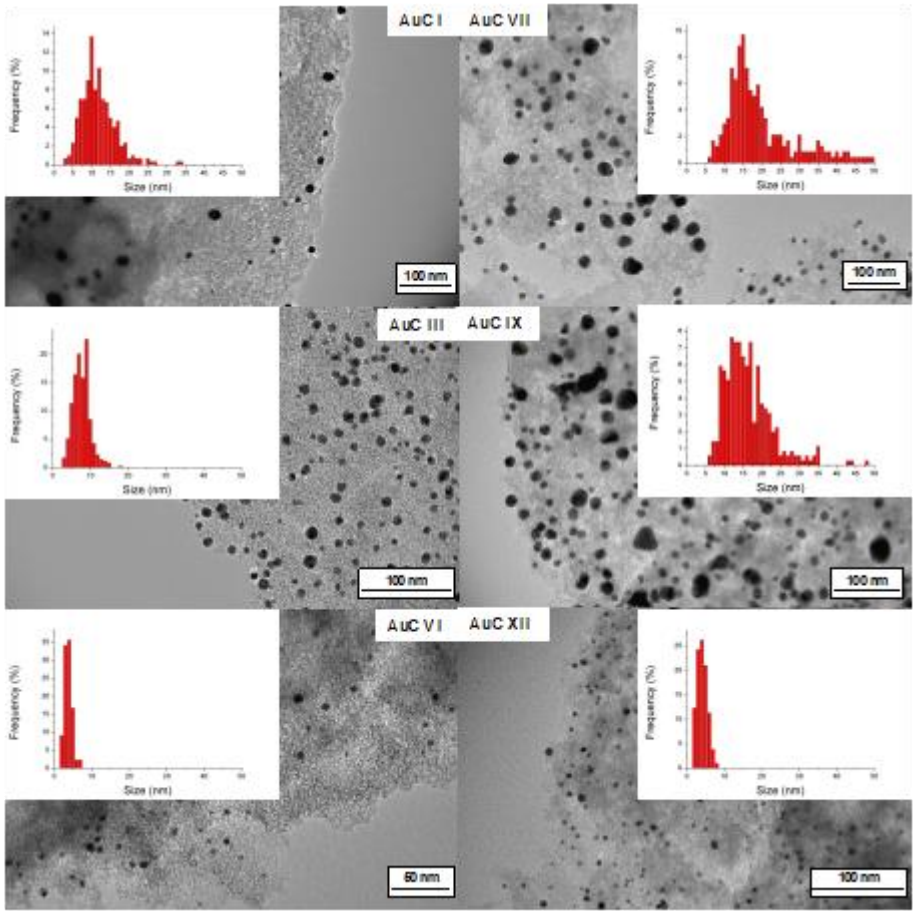

Figure 3. Representative TEM micrographs and gold size distribution for selected Au/C catalysts

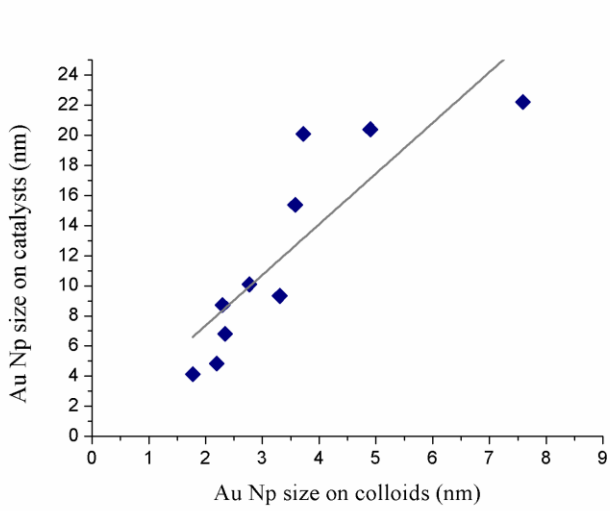

Figure 4. Correlation between the average gold particle size in the colloids and in the corresponding prepared Au/C catalysts.

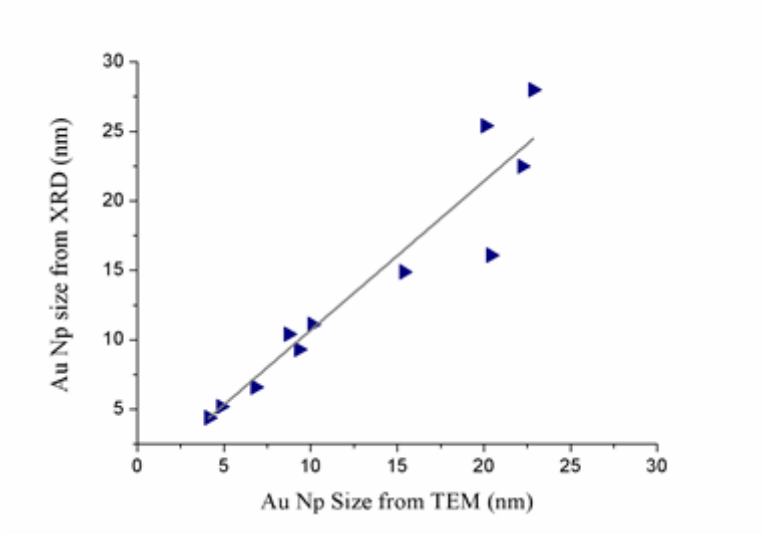

Figure 5. Correlation between the average gold particle size determined by TEM and XRD

In summary, the immobilization of the pre-formed colloids resulted in a series of Au/C catalysts with average gold particle sizes ranging from 4 to 20 nm. Most of the samples presented a similar gold contents (close to 2% wt) and gold particle shape (spherical), with a narrow gold size distribution, and thus, can be used to determine the influence of the gold particle size on the catalytic oxidation of glucose. Only samples prepared at high PVA/Au ratios (>3) or very low $NaBH_4$:Au ratio (<1) must be carefully analyzed, due to, respectively, their lower gold content or different gold particles shape and wide size distribution.

3.3 Catalytic screening

The catalytic activity in terms of glucose conversion of all synthesized Au/C catalysts as a function of the average gold particle size determined from TEM are shown in Figure 6. All samples showed 100 % of selectivity to gluconic acid without formation of other products. Excluding the samples with a significant lower gold content and different gold particle shape and wide size distribution (in red), a linear trend, almost constant, is

observed. The trend is a bit in decline, which could indicate that small gold particles are more active than big ones, which is a general conclusion for gold catalysis [50]. In fact, a maximum in activity for particles around 9 nm is observed, in agreement with the findings of Prati et al. during the last decade and resumed in a recent publication [30]. They found 7 nm as optimal gold nanoparticle size for the highest activity and assigned it to the exercised embedding effect of carbon on smaller nanoparticles.

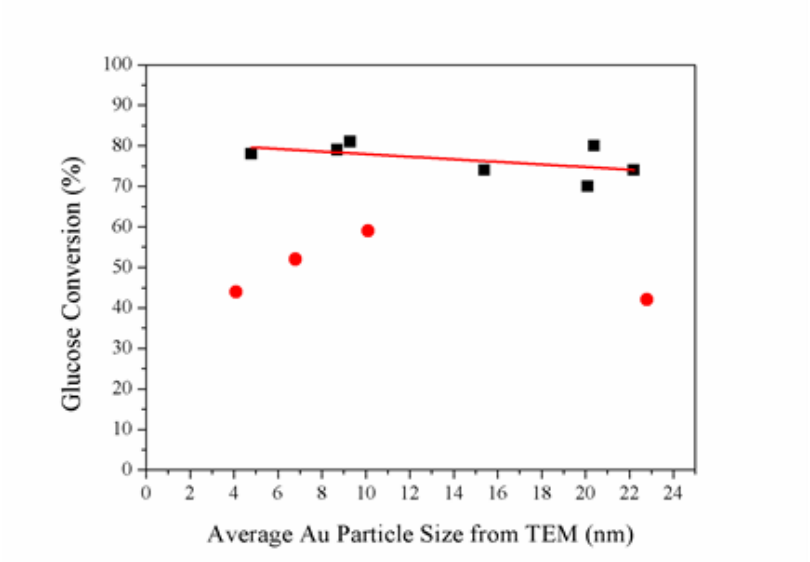

Figure 6. Glucose conversion as a function of the average gold particle size determined by TEM (0.1 MPa O_2, 40ºC, 18h)

Nevertheless if the activity is normalized to the exposed gold surface by using turn-over-frequency (TOF) values (TOF = $\frac{moles\ Glucose\ converted}{moles\ Au*s*dispersion}$) calculated taking into account the gold dispersion estimated from the average gold particle size deduced from TEM and mathematically modeled for cuboctahedral particles [51] and the real Au contents measured from ICP (see table 3), the observed size/activity relationship is somehow different, Figure 7.

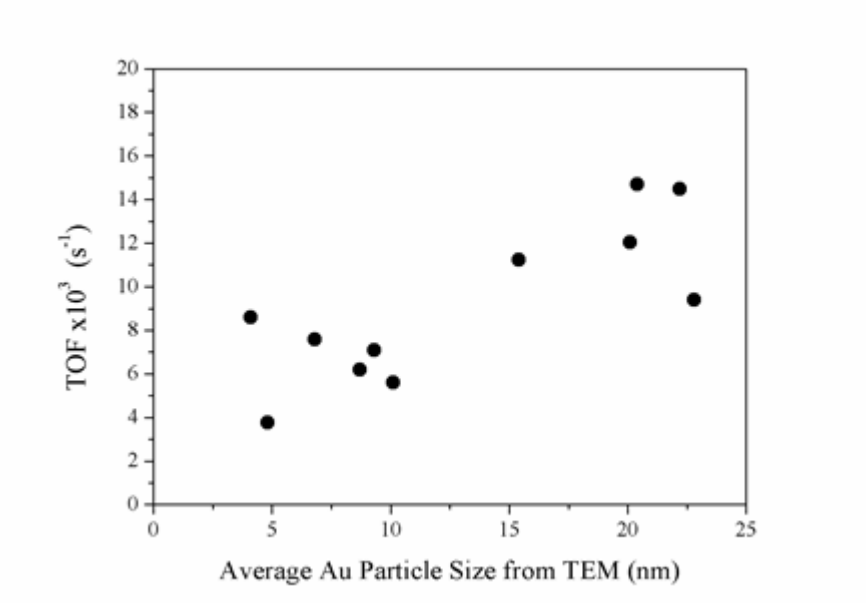

Figure 7. Glucose oxidation turn-over-frequency (TOF) values as a function of the average gold particle size determined from TEM (0.1 MPa O_2, 40ºC, 18h)

Now, the samples could be organized in two groups, samples up to 10 nm showing similar trend and samples with particle size around 15-20 showing superior activity. This result appears somehow contradictory as we consider that higher the particle size lower the gold atoms surface exposure. Anyway, this result suggests that glucose adsorption step should play an important role in the reaction mechanism. And that the adsorption strength and activation mechanism are probably different on small and big size gold particles. In this sense, there is lack of studies considering the reaction mechanism in base-free glucose oxidation conditions. In alkaline conditions, Ishimoto et al. [52] proposed 4 steps theoretical mechanism, where i) glucose is adsorbed on OH adsorbed on Au, ii) OH^- from the solution react with the CHO group of glucose to iii) form and release water by proton transfer and finally iv) gluconic acid is formed by OH transfer from the Au surface. However in base-free conditions the mechanism should occur in a different way. Normally is considered that the liquid phase oxidation of alcohols and aldehydes adopts the commonly known oxidative dehydrogenation mechanism [53] where the reactives are

deprotonated on the metal surface with metal hydrate formation, which subsequently reacts with dissociatively adsorbed oxygen to form water. However, for this mechanism the structure/size dependency is the opposite of that observed in our study, i.e. lower the particle size higher the adsorption/hydrogenation of the CHO group and higher the activity toward acid formation. Taking into account both mechanisms one can consider the adsorption of glucose over metal as the important first step of reaction. Indeed, the energy of adsorption of glucose directly on Au was calculated stronger than that of OH on the same metal [54]. On the other hand, the interaction between activated carbon and Au proceeds through electron transfer from carbon to the metal, inferring slightly negative charge on gold. It was reported, that negatively charged gold clusters easily dissociate oxygen [55]. Taking into account the later the formation of secondary active sites AuO- could be envisaged as the sites able to deprotonate CHO glucose group forming Au-OH, which finally react to form gluconic acid

It is also the place to consider the role of carbon in the reaction. The activated carbon possess a diversity of oxygen containing group being the more important the phenolic groups which could influence by itself or when situated in vicinity of gold particle the apparent reaction rate. Our blank test (using only activated carbon in the same reaction conditions) show 8% of glucose disappearing but without any detectable product formation, suggesting only glucose adsorption on the catalyst surface at this temperature. The reference sample AuC III, with an average gold size of 8.7 nm was selected for the recycling study. Four successive runs were carried out, with Glucose to catalyst ratio kept constant (Figure 8).

The 2^{nd} run presents of around 15 % of activity loss which is half recuperated in the 3^{rd} cycle and stabilized in the 4^{th} one. The variation within the last 3 cycles and especially the loss of activity in the 2^{nd} cycle could be due either to difference in the glucose

adsorption coverage or to its adsorption/desorption equilibrium at this temperature and material.

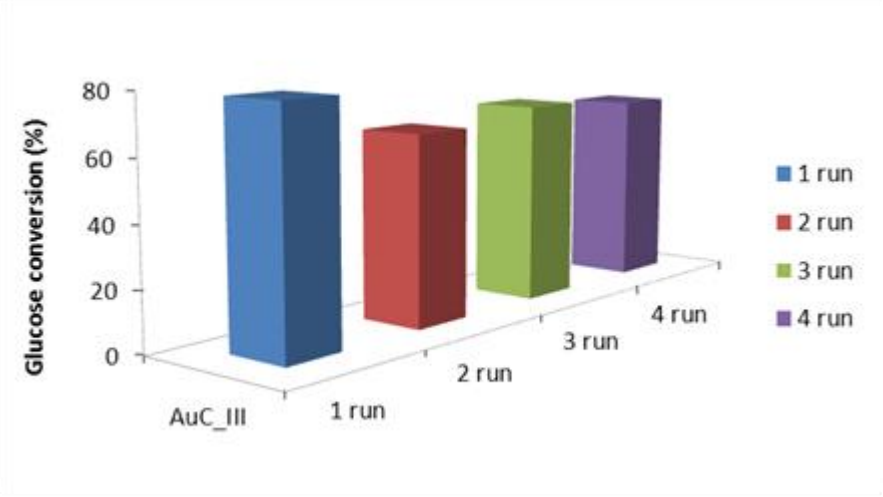

Figure 8. Glucose conversion under recycle runs

4 Conclusions

Gold colloids particle size is influenced by the stabilizing agent and reducing agent/Au ratio. Two limiting values were found in order to achieve stable colloid and homogeneous particles size distribution, the PVA/Au ratio should be superior to 0.85 and $NaBH_4$/Au superior to 3.

The immobilization of the colloids on the carbon support surface was effective. After the calcination treatment, an increment in the average gold particle size was observed, although a good correlation between colloids and supported gold particle sizes was maintained.

With that strategy, we have successfully prepared a series of Au/C samples with similar gold contents (close to 2% wt), gold particle shape (spherical) and narrow gold size distribution, in which the influence of the gold particle size in the catalytic oxidation of glucose could be evaluated.

All catalysts show very good activity in the oxidation of glucose under base free mild conditions with a 100% selectivity to the desired product gluconic acid. The structure/size sensitivity shows optimal size for maximum conversion for particles of around 9 nm, although the normalization to exposed surface gold atoms (TOF) moves this optimum to gold particles in the 15-20 nm range, pointing to a possible influence of the glucose adsorption step in the reaction mechanism.

The catalysts show a very good recyclability with the loss of activity of only 10% after the 4th cycle.

Acknowledgements

Financial support for this work has been obtained from the Spanish Ministerio de Economía y Competitividad (MINECO) (ENE2013-47880-C3-2-R) co-financed by FEDER funds from the European Union. J.L. Santos also acknowledges the same Spanish Ministerio de Economía y Competitividad for his predoctoral fellowship (BES-2014-068244).

Bibliography

[1] D. Carpenter, T.L. Westover, S. Czernik, W. Jablonski, Biomass feedstocks for renewable fuel production: a review of the impacts of feedstock and pretreatment on the yield and product distribution of fast pyrolysis bio-oils and vapors, Green Chem. 16 (2014) 384–406. doi:10.1039/C3GC41631C.

[2] M. Yabushita, H. Kobayashi, A. Fukuoka, Catalytic transformation of cellulose into platform chemicals, Appl. Catal. B Environ. 145 (2014) 1–9. doi:10.1016/j.apcatb.2013.01.052.

[3] M.J. Climent, A. Corma, S. Iborra, Converting carbohydrates to bulk chemicals

and fine chemicals over heterogeneous catalysts, Green Chem. 13 (2011) 520. doi:10.1039/c0gc00639d.

[4] A. Corma Canos, S. Iborra, A. Velty, Chemical routes for the transformation of biomass into chemicals, Chem. Rev. 107 (2007) 2411–2502. doi:10.1021/cr050989d.

[5] J. Song, H. Fan, J. Ma, B. Han, Conversion of glucose and cellulose into value-added products in water and ionic liquids, Green Chem. 15 (2013) 2619–2635. doi:10.1039/C3GC41141A.

[6] S. Hu, Z. Zhang, J. Song, Y. Zhou, B. Han, Efficient conversion of glucose into 5-hydroxymethylfurfural catalyzed by a common Lewis acid SnCl4 in an ionic liquid, Green Chem. 11 (2009) 1746. doi:10.1039/b914601f.

[7] B. Kusserow, S. Schimpf, Claus, Hydrogenation of Glucose to Sorbitol over Nickel andRuthenium Catalysts, Adv. Synth. Catal. 345 (2003) 289–299.

[8] Y. Román-Leshkov, M. Moliner, J. a. Labinger, M.E. Davis, Mechanism of glucose isomerization using a solid lewis acid catalyst in water, Angew. Chemie - Int. Ed. 49 (2010) 8954–8957. doi:10.1002/anie.201004689.

[9] R. Karinen, K. Vilonen, M. Niemelä, Biorefining: Heterogeneously Catalyzed Reactions of Carbohydrates for the Production of Furfural and Hydroxymethylfurfural, ChemSusChem. 4 (2011) 1002–1016. doi:10.1002/cssc.201000375.

[10] U. Prüße, M. Herrmann, C. Baatz, N. Decker, Gold-catalyzed selective glucose oxidation at high glucose concentrations and oxygen partial pressures, Appl. Catal. A Gen. 406 (2011) 89–93. doi:10.1016/j.apcata.2011.08.013.

[11] E.S. H. Hustede, H.J. Haberstroh, Ullmann's Encyclopedia of Industrial Chemistry, 1989.

[12] K. Marcincinova-benabdillah, M. Boustta, J. Coudane, M. Vert, Novel Degradable Polymers Combining D -Gluconic Acid , a Sugar of Vegetal Origin , with Lactic and Glycolic Acids, Biomacromolecules. 76 (2001) 1279–1284.

[13] S. Ramachandran, P. Fontanille, A. Pandey, C. Larroche, Gluconic Acid : Properties , Applications and Microbial Production, Food Technol. Biotechnol. 44 (2006) 185–195.

[14] K. Buchholz, J. Seibel, Industrial carbohydrate biotransformations, Carbohydr. Res. 343 (2008) 1966–1979. doi:10.1016/j.carres.2008.02.007.

[15] Y. Cao, X. Liu, S. Iqbal, P.J. Miedziak, J.K. Edwards, R.D. Armstrong, et al., Base-free oxidation of glucose to gluconic acid using supported gold catalysts, Catal. Sci. Technol. 6 (2015) 107–117. doi:10.1039/C5CY00732A.

[16] C. Megías-Sayago, C.J. Carrasco, S. Ivanova, F.J. Montilla, A. Galindo, J.A. Odriozola, Influence of the ionic liquid presence on the selective oxidation of glucose over molybdenum based catalysts, Catal. Today. In press (2016). doi:10.1016/j.cattod.2016.06.040.

[17] R. Saliger, N. Decker, U. Prüße, D-Glucose oxidation with H2O2 on an Au/Al2O3 catalyst, Appl. Catal. B Environ. 102 (2011) 584–589. doi:10.1016/j.apcatb.2010.12.042.

[18] I. Witońska, M. Frajtak, S. Karski, Selective oxidation of glucose to gluconic acid over Pd-Te supported catalysts, Appl. Catal. A Gen. 401 (2011) 73–82. doi:10.1016/j.apcata.2011.04.046.

[19] a. M. Velarde, P. Bartl, T.E.W. Nießen, W.F. Hoelderich, Hydrogen peroxide oxidation of D-glucose with titanium-containing zeolites as catalysts, J. Mol. Catal. A Chem. 157 (2000) 225–236. doi:10.1016/S1381-1169(00)00073-X.

[20] S. Biella, L. Prati, M. Rossi, Selective Oxidation of D-Glucose on Gold Catalyst,

J. Catal. 206 (2002) 242–247. doi:10.1006/jcat.2001.3497.

[21] Y. Önal, Structure sensitivity and kinetics of ?-glucose oxidation to ?-gluconic acid over carbon-supported gold catalysts, J. Catal. 223 (2004) 122–133. doi:10.1016/j.jcat.2004.01.010.

[22] P. Qi, S. Chen, J. Chen, J. Zheng, X. Zheng, Y. Yuan, Catalysis and Reactivation of Ordered Mesoporous Carbon-Supported Gold Nanoparticles for the Base-Free Oxidation of Glucose to Gluconic Acid, ACS Catal. 5 (2015) 2659–2670. doi:10.1021/cs502093b.

[23] C. Kooyman, K. Vellenga, H.G.J.D.E. Wilt, Carbohydrate Research, 54 (1977) 33-44 ©, 54 (1977) 33–44.

[24] M. Comotti, C. Della Pina, R. Matarrese, M. Rossi, The catalytic activity of "naked" gold particles, Angew. Chemie - Int. Ed. 43 (2004) 5812–5815. doi:10.1002/anie.200460446.

[25] P. Beltrame, M. Comotti, C. Della Pina, M. Rossi, Aerobic oxidation of glucose, Appl. Catal. A Gen. 297 (2006) 1–7. doi:10.1016/j.apcata.2005.08.029.

[26] T. Ishida, N. Kinoshita, H. Okatsu, T. Akita, T. Takei, M. Haruta, Influence of the Support and the Size of Gold Clusters on Catalytic Activity for Glucose Oxidation, Angew. Chemie Int. Ed. 47 (2008) 9265–9268. doi:10.1002/anie.200802845.

[27] X. Cao, X. Peng, S. Sun, L. Zhong, W. Chen, S. Wang, et al., Hydrothermal conversion of xylose, glucose, and cellulose under the catalysis of transition metal sulfates, Carbohydr. Polym. 118 (2015) 44–51. doi:10.1016/j.carbpol.2014.10.069.

[28] Y. Wang, S. Van de Vyver, K.K. Sharma, Y. Román-Leshkov, Insights into the stability of gold nanoparticles supported on metal oxides for the base-free

oxidation of glucose to gluconic acid, Green Chem. 16 (2014) 719–726. doi:10.1039/C3GC41362D.

[29] C. Megías-Sayago, S. Ivanova, M.A. Centeno, J.A. Odriozola, Gold catalysts screening in base-free aerobic oxidation of glucose to gluconic acid, Catal. Today. In press (2016). doi:10.1016/j.cattod.2016.06.046.

[30] L. Prati, A. Villa, A.R. Lupini, G.M. Veith, Gold on carbon: one billion catalysts under a single label, Phys. Chem. Chem. Phys. 14 (2012) 2969. doi:10.1039/c2cp23405j.

[31] P.J. Miedziak, H. Alshammari, S. a. Kondrat, T.J. Clarke, T.E. Davies, M. Morad, et al., Base-free glucose oxidation using air with supported gold catalysts, Green Chem. 16 (2014) 3132. doi:10.1039/c4gc00087k.

[32] H. Okatsu, N. Kinoshita, T. Akita, T. Ishida, M. Haruta, Deposition of gold nanoparticles on carbons for aerobic glucose oxidation, Appl. Catal. A Gen. 369 (2009) 8–14. doi:10.1016/j.apcata.2009.08.013.

[33] Y. Önal, S. Schimpf, P. Claus, Structure sensitivity and kinetics of D-glucose oxidation to D-gluconic acid over carbon-supported gold catalysts, J. Catal. 223 (2004) 122–133. doi:10.1016/j.jcat.2004.01.010.

[34] H.F. Cui, J.S. Ye, X. Liu, W.D. Zhang, F.S. Sheu, Pt-Pb alloy nanoparticle/carbon nanotube nanocomposite: a strong electrocatalyst for glucose oxidation, Nanotechnology. 17 (2006) 2334–39. doi:10.1088/0957-4484/17/9/043.

[35] L. Prati, M. Rossi, Gold on carbon as a new catalyst for selective liquid phase oxidation of diols, J. Catal. 176 (1998) 552–560. doi:DOI 10.1006/jcat.1998.2078.

[36] S. Gil, L. Muñoz, L. Sánchez-Silva, A. Romero, J.L. Valverde, Synthesis and

characterization of Au supported on carbonaceous material-based catalysts for the selective oxidation of glycerol, Chem. Eng. J. 172 (2011) 418–429. doi:10.1016/j.cej.2011.05.108.

[37] C. Della Pina, E. Falletta, Gold-catalyzed oxidation in organic synthesis: a promise kept, Catal. Sci. Technol. 1 (2011) 1564. doi:10.1039/c1cy00283j.

[38] I. V. Delidovich, B.L. Moroz, O.P. Taran, N. V. Gromov, P. a. Pyrjaev, I.P. Prosvirin, et al., Aerobic selective oxidation of glucose to gluconate catalyzed by Au/Al2O3 and Au/C: Impact of the mass-transfer processes on the overall kinetics, Chem. Eng. J. 223 (2013) 921–931. doi:10.1016/j.cej.2012.11.073.

[39] C. Bianchi, S. Biella, A. Gervasini, L. Prati, M. Rossi, Gold on carbon: influence of support properties on catalyst activity in liquid-phase oxidation, Catal. Letters. 85 (2003) 91–96. doi:10.1023/A:1022176909660.

[40] F. Rodriguez-Reinoso, The role of carbon materials in heterogeneous catalalysis, Carbon N. Y. 36 (1998) 159–175.

[41] J.H. Vleeming, B.F.M. Kuster, G.B. Marin, Effect of platinum particle size and catalyst support on the platinum catalyzed selective oxidation of carbohydrates, Catal. Letters. 46 (1997) 187–194.

[42] K.C. Ruthiya, J. van der Schaaf, B.F.M. Kuster, J.C. Schouten, Modeling the effect of particle-to-bubble adhesion on mass transport and reaction rate in a stirred slurry reactor: influence of catalyst support, Chem. Eng. Sci. 59 (2004) 5551–5558.

[43] J. Luo, W. Chu, S. Sall, C. Petit, Facile synthesis of monodispersed Au nanoparticles-coated on Stöber silica, Colloids Surfaces A Physicochem. Eng. Asp. 425 (2013) 83–91. doi:10.1016/j.colsurfa.2013.02.056.

[44] P. Bera, M.S. Hedge, No Title, Catal. Letters. 79 (2002) 107.

[45] G.C. Bond, D.T. Thompson, Catalysis by Gold, Catal. Rev. Sci. Eng. 41 (1999) 319–388. doi:10.1081/CR-100101171.

[46] J. Polte, Fundamental Growth Principles of Colloidal Metal Nanoparticles - a new Perspective, CrystEngComm. 17 (2015) 6809–6830. doi:10.1039/C5CE01014D.

[47] X. Ji, X. Song, J. Li, Y. Bai, W. Yang, Size Control of Gold Nanocrystals in Citrate Reduction : The Third Role of Citrate, (2007) 1957–1962.

[48] S. Ivanova, V. Pitchon, C. Petit, H. Herschbach, A. Van Dorsselaer, E. Leize, Preparation of alumina supported gold catalysts: Gold complexes genesis, identification and speciation by mass spectrometry, Appl. Catal. A Gen. 298 (2006) 203–210. doi:10.1016/j.apcata.2005.10.018.

[49] N.T.K. Thanh, N. Maclean, S. Mahiddine, Mechanisms of Nucleation and Growth of Nanoparticles in Solution, Chem Rev. 3 (2014) 7610.

[50] M. Haruta, Gold as a novel catalyst in the 21st century: Preparation, working mechanism and applications, Gold Bull. 37 (2004) 27–36.

[51] S. Ivanova, V. Pitchon, C. Petit, Application of the direct exchange method in the preparation of gold catalysts supported on different oxide materials, J. Mol. Catal. A Chem. 256 (2006) 278–283. doi:10.1016/j.molcata.2006.05.006.

[52] T. Ishimoto, Y. Hamatake, H. Kazuno, T. Kishida, M. Koyama, Theoretical study of support effect of Au catalyst for glucose oxidation of alkaline fuel cell anode, Appl. Surf. Sci. 324 (2015) 76–81. doi:10.1016/j.apsusc.2014.10.125.

[53] T. Mallat, A. Baiker, No TitleOxidation of alcohols with molecular oxygen on platinum metal catalysts in aqueous solutions, Catal. Today. 19 (1994) 247–284.

[54] T. Ishimoto, H. Kazuno, T, Kishida, M. Koyama, No Title, Solid State Ionics. 262 (2014) 328–331.

[55] A. Franceschetti, S.J. Pennycook, S.T. Pantelides, Oxygen chemisorption on Au nanoparticles, Chem. Phys. Lett. 374 (2003) 471–475. doi:10.1016/S0009-2614(03)00725-5.